

Dynamic ultrasound radiation force in fluids

Glauber T. Silva*

*Departamento de Tecnologia da Informação, Universidade Federal de Alagoas,
BR 104, km 14, Tabuleiro dos Martins, Maceió, AL, Brazil, 57072-970.*

Shigao Chen, James F. Greenleaf, and Mostafa Fatemi

*Department of Physiology and Biomedical Engineering,
Mayo Clinic College of Medicine, 200 1st St. SW, Rochester, MN, USA, 55905.*

(Dated: November 19, 2018)

The subject of this paper is to present a theory for the dynamic radiation force produced by dual-frequency ultrasound beams in lossless and non-dispersive fluids. A formula for the dynamic radiation force exerted on a three-dimensional object by a dual-frequency beam is obtained stemming from the fluid dynamics equations. Dependence of the dynamic radiation force to nonlinear effects of the medium is analyzed. The developed theory is applied to calculate the dynamic radiation force exerted on solid elastic (brass and stainless steel) spheres by a low-amplitude dual-frequency plane wave. The dynamic radiation force is calculated by solving the dual-frequency plane wave scattering problem for solid elastic spheres. Results show that the dynamic radiation force on the analyzed spheres presents fluctuations similar to those present in the static radiation force. Furthermore, analysis of the static and the dynamic radiation forces on the stainless steel sphere shows that they have approximately the same magnitude.

PACS numbers: 43.25.+y, 43.35.+d

I. INTRODUCTION

It is known that acoustic waves carry momentum. When an acoustic wave strikes an object, part of its momentum is transferred to the object giving rise to the acoustic radiation force phenomenon [1, 2, 3, 4]. Acoustic radiation force has found practical importance in many applications. For example, measure the power output of transducers in medical ultrasound machines [5], ultrasound radiometer [6], liquid drops levitation [7], and motion of gas bubbles in liquids [8].

In these applications, the radiation force is static, being generated by a continuous-wave (CW) ultrasound beam. Time-dependent (dynamic) ultrasound radiation force can also be produced by amplitude-modulated (AM) or pulsed ultrasound beams. In general, an AM beam produces a harmonic radiation force at the modulation frequency, while a pulsed beam generates a pulsed radiation force. Dynamic radiation force has been applied for measuring the ultrasound power of transducers using a disk target [9] or a shaped-wedge vane [10], and determining ultrasound absorption coefficient in liquids [11].

In recent years, dynamic ultrasound radiation force has become of practical importance in elastography; specifically in the following imaging techniques:

- Acoustic radiation force impulse imaging (ARFI) uses pulsed ultrasound radiation force to produce displacement in tissue which is detected to form an image of the tissue [12].
- Shear wave elasticity imaging (SWEI) images tissue properties by detecting shear acoustic waves induced by the harmonic ultrasound radiation force produced by an AM ultrasound beam [13].
- Vibro-acoustography maps the mechanical response of an object to a harmonic ultrasound radiation force produced by two overlapping CW ultrasound beams whose frequencies are slightly different [14, 15]. In this context, it has been demonstrated that viscoelastic properties of gel phantoms can be accurately determined by measuring the amplitude of vibration induced by the dynamic ultrasound radiation force on a small sphere embedded in the medium [16].

*Electronic address: glauber@tci.ufal.br

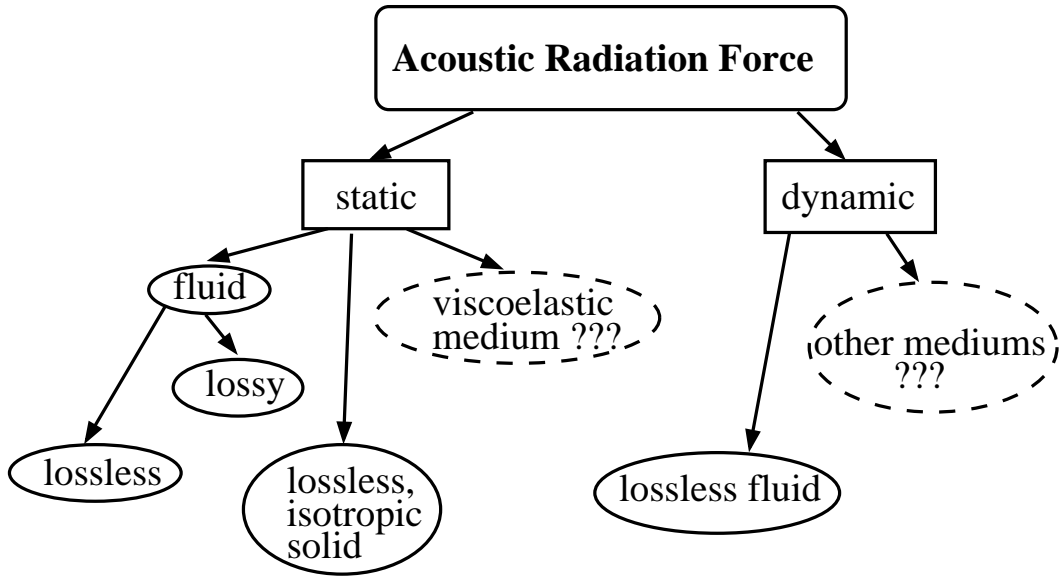


FIG. 1: Diagram showing the theory of acoustic radiation force in different propagating mediums. Dashed ellipses show the lack of theory for acoustic radiation force.

Lord Rayleigh was the first to propose a theory for acoustic radiation force in lossless fluids due to compressional waves [17]. Static radiation force in lossy fluids has been studied by Jiang *et al.* [18], Doinikov [19], and Danilov *et al.* [20]. A study of the static radiation force in lossless isotropic elastic solid can be seen in Ref [21]. Usually the radiation force exerted on an object target by a CW ultrasound can be obtained by solving the vector surface integral of the radiation-stress tensor (defined as the time-average of the wave momentum flux) over a surface enclosing the object. The radiation-stress is obtained in terms of the incident beam and the scattered field by the object. Several authors derived the static radiation force, by solving the scattering problem of CW plane waves by spherical or cylindrical objects [22, 23, 24, 25, 26, 27, 28]. Most studies realized for the dynamic radiation force have been focused on finding applications to it. No theoretical efforts to tackle the problem of dynamic ultrasound radiation force exerted on an embedded object in a medium have been made whatsoever. Figure 1 depicts the theoretical realm of acoustic radiation force. This figure includes the contribution of this paper: dynamic radiation force in lossless fluids. Dashed ellipses show the lack of theoretical models for acoustic radiation force.

The increasing applications of dynamic radiation force of ultrasound in elastography techniques prompted us to develop a method to calculate this force. Here, we present a theory of dynamic ultrasound radiation force exerted on arbitrary shaped three-dimensional objects. The theory is restricted to the radiation force produced by dual-frequency CW ultrasound waves in lossless fluids. In what follows, we briefly discuss the dynamic equations of lossless fluids in Sec. II A. In Sec. II B, we present a theory of ultrasound radiation force. We obtain a formula for the dynamic ultrasound radiation force exerted on an object by a dual-frequency CW ultrasound wave. The formula is given in terms of a vector surface integral of the wave velocity potential over the object's surface. Explicit dependence of the dynamic radiation force with the medium nonlinearity is pointed out. In Sec. III, we apply the theory to calculate the dynamic ultrasound radiation force exerted on solid elastic (brass and stainless steel) spheres. Finally, in Sec. IV we summarize the main results of this paper.

II. THEORY

A. Dynamics of lossless fluids

Consider a homogeneous isotropic fluid in which thermal conductivity and viscosity are neglected. This corresponds to the so-called ideal fluid. The medium is characterized by the following acoustic fields: pressure p , density ρ , and particle velocity \mathbf{v} . Here all acoustic fields are functions of the position vector $\mathbf{r} \in \mathbb{R}^3$ and time $t \in \mathbb{R}$. In an initial state without sound perturbation these quantities assume constant values given by $p = p_0$, $\rho = \rho_0$, and $\mathbf{v} = 0$. The quantity $p - p_0$ is the excess of pressure in the medium. The equations that describe the dynamic

of ideal fluids can be derived from conservation principles for mass, momentum, and thermodynamic equilibrium. These equations, neglecting effects of gravity, are presented here as follows [29]:

$$\frac{\partial \rho}{\partial t} + \nabla \cdot (\rho \mathbf{v}) = 0, \quad (1)$$

$$\rho \frac{d\mathbf{v}}{dt} = -\nabla p, \quad (2)$$

$$p = p_0 \left(\frac{\rho}{\rho_0} \right)^{(1+B/A)}, \quad (3)$$

where ∇ is the gradient operator, the symbol \cdot stands for the scalar product, and B/A is the Fox-Wallace parameter [30] which characterizes the nonlinearity of the fluid. Equations (1)-(3) form a system of nonlinear partial differential equations that gives a full description of the wave propagation in the fluid. The conservation of fluid mass is represented by Eq. (1). Equation (2) is a version of the Newton's second-law in fluid dynamics. Equation (3) is an adiabatic equation of state known as Tait's equation.

A lossless fluid is irrotational. Thus, according to the Helmholtz vector theorem, the particle velocity can be expressed in terms of the velocity potential function ϕ as

$$\mathbf{v} = -\nabla \phi. \quad (4)$$

The velocity potential can be expanded as a sum of a linear term and higher-order contributions as follows

$$\phi = \phi^{(1)} + \phi^{(2)} + \dots \quad (5)$$

where $\phi^{(1)}$ and $\phi^{(2)}$ are the linear and the second-order velocity potentials, respectively. In terms of the linear velocity potential, the linear pressure and velocity fields are given by

$$p^{(1)} = \rho_0 \frac{\partial \phi^{(1)}}{\partial t}, \quad (6)$$

$$\mathbf{v}^{(1)} = -\nabla \phi^{(1)}. \quad (7)$$

B. Instantaneous net force

A volume element in a fluid is subject to a stress caused by the sound wave propagation throughout it. Stresses caused by sound perturbation in the fluid should be described by Eq. (2).

Consider an ultrasound beam striking a homogeneous object of finite extension and surface S_0 at rest. As the ultrasound field hits the object, its surface may be deformed and dislocated. We denote the object's surface at the time t by S . Fig. 2 depicts the interaction between the incident ultrasound wave and the object target.

The instantaneous net force \mathbf{f} acting on the object is obtained by integrating Eq. (2) on the object's volume. Since the ambient pressure p_0 does not contribute to the net force on the object, we can replace p by $p - p_0$ in Eq. (2). Hence, integrating Eq. (2) on the object's volume and using the Gauss' integral theorem, we obtain

$$\mathbf{f} = - \int_S (p - p_0) \mathbf{n} dS, \quad (8)$$

where \mathbf{n} is the outward normal unit-vector of the integration surface.

Radiation force is a phenomenon that depends on the interaction of second-order acoustic fields with the object target. To avoid the integration of $p - p_0$ over the time-dependent object's surface S , we need to find $p - p_0$ up to second-order. The idea is to replace S by S_0 for second-order integrands in Eq. (8). For first-order integrands, we should keep S and analyze the contribution of the integral to the radiation force. From Eqs. (1) - (3), one can show that the second-order excess of pressure is given by [31]

$$p - p_0 = \rho_0 \left(\frac{\partial \phi^{(1)}}{\partial t} + \frac{\partial \phi^{(2)}}{\partial t} \right) + \frac{p^{(1)2}}{2\rho_0 c_0^2} - \frac{\rho_0 \mathbf{v}^{(1)} \cdot \mathbf{v}^{(1)}}{2}, \quad (9)$$

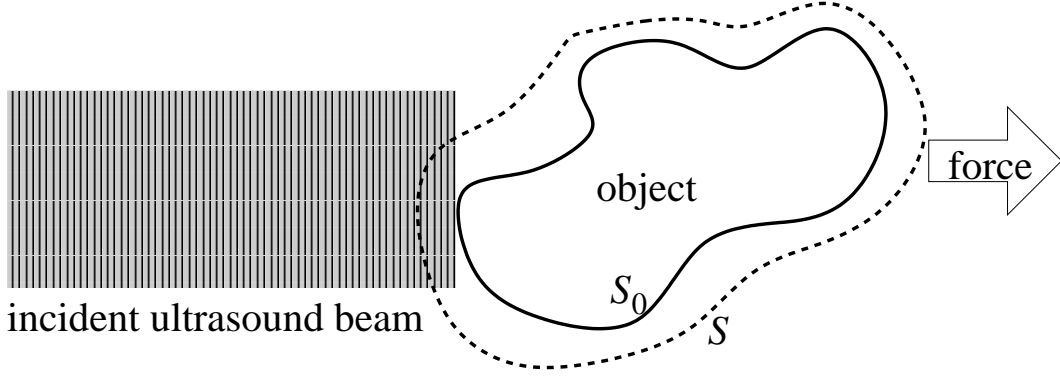


FIG. 2: Net force exerted on an object by an ultrasound beam. The dotted contour depicts changes on the object's surface.

where c_0 is the small-amplitude speed of sound. Substituting Eq. (9) into Eq. (8) and holding terms up to second-order, we find

$$\mathbf{f} = -\rho_0 \int_S \frac{\partial \phi^{(1)}}{\partial t} \mathbf{n} dS - \rho_0 \int_{S_0} \frac{\partial \phi^{(2)}}{\partial t} \mathbf{n} dS - \frac{1}{2\rho_0 c_0^2} \int_{S_0} p^{(1)2} \mathbf{n} dS + \frac{\rho_0}{2} \int_{S_0} (\mathbf{v}^{(1)} \cdot \mathbf{v}^{(1)}) \mathbf{n} dS. \quad (10)$$

By using the relation [23]

$$\int_S \frac{\partial \phi^{(1)}}{\partial t} \mathbf{n} dS = \frac{d}{dt} \int_S \phi^{(1)} \mathbf{n} dS + \int_S (\mathbf{n} \cdot \mathbf{v}^{(1)}) \mathbf{v}^{(1)} dS$$

in Eq. (10) and again keeping up to the second-order terms, we get

$$\mathbf{f} = -\rho_0 \frac{d}{dt} \left(\int_S \phi^{(1)} \mathbf{n} dS + \int_{S_0} \phi^{(2)} \mathbf{n} dS \right) - \int_{S_0} \mathbf{n} \cdot \mathbf{T} dS. \quad (11)$$

We call the quantity \mathbf{T} as the radiation-stress tensor. It is given by

$$\mathbf{T} \equiv \left[\frac{p^{(1)2}}{2\rho_0 c_0^2} - \frac{\rho_0 (\mathbf{v}^{(1)} \cdot \mathbf{v}^{(1)})}{2} \right] \mathbf{I} + \rho_0 \mathbf{v}^{(1)} \mathbf{v}^{(1)}, \quad (12)$$

where \mathbf{I} is the 3×3 -unit matrix and $\rho_0 \mathbf{v}^{(1)} \mathbf{v}^{(1)}$ is a dyad [32] known as the Reynolds' stress. We have written down Eq. (12) using the identities $\mathbf{n} \cdot \mathbf{v}^{(1)} \mathbf{v}^{(1)} = (\mathbf{n} \cdot \mathbf{v}^{(1)}) \mathbf{v}^{(1)}$ and $\mathbf{n} \cdot \mathbf{I} = \mathbf{n}$.

Consider g as a function of time. The Fourier transform of g is defined as

$$\hat{g}(\omega) = \mathcal{F}[g] \equiv \int_{-\infty}^{+\infty} g(t) e^{-j\omega t} dt,$$

where ω (angular frequency) is the reciprocal variable of t and j is the imaginary-unit. To analyze the frequency components present in the net of force, we take the Fourier transform of Eq. (11) as follows

$$\hat{\mathbf{f}}(\omega) = -j\omega \rho_0 \mathcal{F} \left[\int_S \phi^{(1)} \mathbf{n} dS \right] - j\omega \rho_0 \int_{S_0} \mathcal{F} [\phi^{(2)}] \mathbf{n} dS - \int_{S_0} \mathbf{n} \cdot \mathcal{F}[\mathbf{T}] dS. \quad (13)$$

This equation gives a description of the frequency spectrum of the net of force acting on the object. We shall use this equation to calculate the static and the dynamic radiation forces.

C. Static radiation force

The static component of the net force \mathbf{f} is commonly known as acoustic radiation force. Here, we call it static radiation force. Acoustic radiation force has been studied as a time averaged force. The rule of the time-average is to isolate the static component ($\omega = 0$) of the net force acting on the object.

Consider an incident ultrasound wave, periodic in time, striking the object target. The static component of the radiation force corresponds to $\omega = 0$ in Eq. (13). The first two integrals in the right-hand side of this equation become zero. Therefore, the static radiation force is

$$\mathbf{f}_s = - \int_{S_0} \mathbf{n} \cdot \mathcal{F}[\mathbf{T}]_{\omega=0} dS.$$

Recognizing that the time-average of \mathbf{T} over a long time interval is $\langle \mathbf{T} \rangle = \mathcal{F}[\mathbf{T}]_{\omega=0}$, we get

$$\mathbf{f}_s = - \int_{S_0} \mathbf{n} \cdot \langle \mathbf{T} \rangle dS. \quad (14)$$

Note that \mathbf{f}_s is a real quantity.

The static radiation force can be understood as follows. The incident ultrasound beam is scattered by the object. The static radiation force is the time averaged rate of the momentum change due to the scattering by the object.

The time-average of the radiation-stress is a zero-divergence quantity, i.e., $\nabla \cdot \langle \mathbf{T} \rangle = 0$ [4]. This means that no static radiation force is present in an ideal fluid if there is no target. Consequently, steady streaming does not happen in lossless fluids [33].

D. Dynamic ultrasound radiation force

In this section, we concentrate on the dynamic radiation force produced by an amplitude-modulated (AM) ultrasound beam. We chose the dynamic ultrasound force produced by AM ultrasound waves because of its importance in elastography; specifically in SWEI and vibro-acoustography. An AM ultrasound wave is described by a carrier f_0 and modulation Δf frequencies. Usually the carrier frequency is much larger than the modulation frequency.

Here, the AM ultrasound beam is produced by two overlapping CW ultrasound beams. We call this beam a “dual-frequency ultrasound beam”. The frequencies of this beam are $f_a = f_0 + \Delta f/2$ and $f_b = f_0 - \Delta f/2$. The corresponding angular frequencies of the beam are $\omega_a = 2\pi f_a$ and $\omega_b = 2\pi f_b$. The frequencies f_0 and Δf are also called the center and the difference frequencies, respectively.

When an object is placed in the wave path, the dual-frequency ultrasound beam is scattered by the object. The first-order velocity potential in the medium is given by

$$\phi^{(1)} = \Re \left\{ \hat{\phi}_a e^{j\omega_a t} + \hat{\phi}_b e^{j\omega_b t} \right\}, \quad (15)$$

where $\Re\{\cdot\}$ is the real-part of a complex quantity. The functions $\hat{\phi}_a$ and $\hat{\phi}_b$ are spatial complex amplitudes of each frequency component of the wave. The amplitude functions in Eq. (15) are given as the sum of the velocity potential amplitudes of the incident and scattered waves.

The radiation force exerted on the object by the dual-frequency beam includes the following components: a static component ($\omega = 0$), a component at the difference frequency $\Delta\omega$, and high-frequency components at $2\omega_a$, $2\omega_b$, and $\omega_a + \omega_b$. In this paper, the component at $\Delta\omega$ is called the dynamic radiation force.

To obtain the static and the dynamic radiation force produced by the dual-frequency ultrasound beam, we calculate the Fourier transform of the radiation stress \mathbf{T} up to the difference frequency $\Delta\omega$. Substituting Eq. (15) into Eq. (12), through Eqs. (6) and (7), and taking the Fourier transform of the result, we obtain the static, $\langle \mathbf{T} \rangle$, and the dynamic, $\hat{\mathbf{T}}_{\Delta\omega}$, radiation-stresses as follows

$$\langle \mathbf{T} \rangle = \langle \mathbf{T}_a \rangle + \langle \mathbf{T}_b \rangle, \quad (16)$$

$$\hat{\mathbf{T}}_{\Delta\omega} = \frac{\rho_0}{2} \left[\left(k_a k_b \hat{\phi}_a \hat{\phi}_b^* - \nabla \hat{\phi}_a \cdot \nabla \hat{\phi}_b^* \right) \mathbf{I} + \nabla \hat{\phi}_a \nabla \hat{\phi}_b^* + \nabla \hat{\phi}_b^* \nabla \hat{\phi}_a \right]. \quad (17)$$

The quantities $\langle \mathbf{T}_a \rangle$ and $\langle \mathbf{T}_b \rangle$ are the averaged radiation-stress of each frequency component of the dual-frequency wave and $k_a = \omega_a/c_0$ and $k_b = \omega_b/c_0$. Explicitly, the averaged radiation-stresses $\langle \mathbf{T}_a \rangle$ and $\langle \mathbf{T}_b \rangle$ are given by

$$\langle \mathbf{T}_m \rangle = \frac{\rho_0}{4} \left(k_m^2 |\hat{\phi}_m|^2 - |\nabla \hat{\phi}_m|^2 \right) \mathbf{I} + \frac{\rho_0}{2} (\nabla \hat{\phi}_m \nabla \hat{\phi}_m^*), \quad m = a, b. \quad (18)$$

Now both the static and dynamic radiation force can be obtained. According to Eq. (14) the static radiation force is

$$\mathbf{f}_s = - \int_{S_0} \mathbf{n} \cdot (\langle \mathbf{T}_a \rangle + \langle \mathbf{T}_b \rangle) dS. \quad (19)$$

Based on Eq. (13) the amplitude (in complex notation) of the dynamic radiation force at $\Delta\omega$ is

$$\hat{\mathbf{f}}_{\Delta\omega} = -j\rho_0\Delta\omega \left\{ \mathcal{F} \left[\int_S \phi^{(1)} \mathbf{n} dS \right]_{\omega=\Delta\omega} + \int_{S_0} \hat{\phi}_{\Delta\omega}^{(2)} \mathbf{n} dS \right\} - \int_{S_0} \mathbf{n} \cdot \hat{\mathbf{T}}_{\Delta\omega} dS. \quad (20)$$

where $\hat{\phi}_{\Delta\omega}^{(2)} = \mathcal{F}[\phi^{(2)}]_{\omega=\Delta\omega}$.

Let us analyze the contribution of the first integral in the right-hand side of Eq. (20). By using the Gauss' integral theorem, this integral can be expressed as

$$\int_S \phi^{(1)} \mathbf{n} dS = - \int_{V_0} \mathbf{v}^{(1)} dV - \int_{\delta V} \mathbf{v}^{(1)} dV,$$

where V_0 is volume of the object at rest and δV is the volume variation of the object induced by the excess of pressure at the time t (see Fig. 2). The first integral in this equation does not have any harmonic term at the difference frequency $\Delta\omega$, thus, by taking the Fourier transform of it and isolating the frequency component $\omega = \Delta\omega$, we obtain

$$\mathcal{F} \left[\int_S \phi^{(1)} \mathbf{n} dS \right]_{\omega=\Delta\omega} = - \mathcal{F} \left[\int_{\delta V} \mathbf{v}^{(1)} dV \right]_{\omega=\Delta\omega}.$$

Inasmuch as the particle velocity is a limited and continuous function inside the volume δV , there exists a point $\mathbf{r}_0 \in \delta V$ such that [34] $\int_{\delta V} \mathbf{v}^{(1)} dV = \delta V \mathbf{v}^{(1)}(\mathbf{r}_0, t)$. Thus, the amplitude of the dynamic radiation force of the first term in Eq. (20) is

$$F_0 = -j\rho_0\Delta\omega \mathcal{F} \left[\int_S \phi^{(1)} \mathbf{n} dS \right]_{\omega=\Delta\omega} = j\Delta\omega \mathcal{F} \left[\delta M \mathbf{v}_0^{(1)} \right]_{\omega=\Delta\omega}, \quad (21)$$

where $\mathbf{v}_0^{(1)} = \mathbf{v}^{(1)}(\mathbf{r}_0, t)$ and $\delta M = \rho_0 \delta V$ corresponds to the fluid mass variation at the time t caused by the object vibration. Therefore, the dynamic radiation force can be written as

$$\begin{aligned} \hat{\mathbf{f}}_{\Delta\omega} &= j\Delta\omega \mathcal{F} \left[\delta M \mathbf{v}_0^{(1)} \right]_{\omega=\Delta\omega} - j\Delta\omega \rho_0 \int_{S_0} \hat{\phi}_{\Delta\omega}^{(2)} \mathbf{n} dS \\ &\quad - \frac{\rho_0}{2} \int_{S_0} \left[\left(k_a k_b \hat{\phi}_a \hat{\phi}_b^* - \nabla \hat{\phi}_a \cdot \nabla \hat{\phi}_b^* \right) \mathbf{n} + (\mathbf{n} \cdot \nabla \hat{\phi}_a) \nabla \hat{\phi}_b^* + (\mathbf{n} \cdot \nabla \hat{\phi}_b^*) \nabla \hat{\phi}_a \right] dS. \end{aligned} \quad (22)$$

Thus, the dynamic radiation force exerted on the object target comes from three different interactions between the ultrasound field and the object. The first term in the right-hand side of Eq. (22) corresponds to momentum rate exchange due to fluid mass variation caused by the object vibration. The next term in this equation accounts for the interaction of the second-order velocity potential with the object target. None of these terms are present on the static radiation force formula (19). The last term in Eq. (22) is related to the interaction of the radiation-stress and the object. We shall apply Eq. (22) to calculate the dynamic radiation force on a solid small sphere.

In time-domain, the dynamic radiation force is given as the inverse Fourier transform of $\hat{\mathbf{f}}_{\Delta\omega}$. Therefore, the dynamic radiation force exerted on a object is given by

$$\mathbf{f}_{\Delta\omega}(t) = \Re \left\{ \hat{\mathbf{f}}_{\Delta\omega} e^{j\Delta\omega t} \right\}. \quad (23)$$

Note that if $\Delta\omega = 0$ and $\hat{\phi}_a = \hat{\phi}_b$, we have $\hat{\mathbf{f}}_{\Delta\omega} = \mathbf{f}_s$. Consequently, the magnitude of both dynamic and static radiation forces becomes equal when $\Delta\omega = 0$.

III. DYNAMIC RADIATION FORCE ON A SOLID SPHERE

A. Linear ultrasound scattering

Consider a collimated dual-frequency plane wave described by Eq. (15) impinging on a solid elastic sphere of radius r_0 localized at the origin of the coordinate system. The beam propagates along the z -axis. The sphere

is characterized by three parameters: density ρ_1 , compressional wave speed c_c , and shear wave speed c_s . The amplitude functions of the incident plus the scattered waves are given, in spherical coordinates, by [35]

$$\hat{\phi}_m = A_0 \sum_{n=0}^{\infty} (2n+1)(-j)^n [j_n(k_m r) + S_{m,n} h_n^{(2)}(k_m r)] P_n(\cos \theta), \quad m = a, b. \quad (24)$$

where A_0 is the magnitude of the incident wave, $k_m = \omega_m/c_0$, j_n is the spherical Bessel function, $S_{m,n}$ is the scattering function determined by boundary conditions, and $h_n^{(2)}$ is the spherical Hankel function of second-kind. The scattering function is given by

$$S_{m,n} = -\frac{D_{m,n} j_n(x_m) - x_m j_n'(x_m)}{D_{m,n} h_n^{(2)}(x_m) - x_m h_n^{(2)'}(x_m)}, \quad m = a, b, \quad (25)$$

where the prime symbol means derivative with respect to the function's argument and $x_m = k_m r_0$. The coefficient $D_{m,n}$ is given by

$$D_{m,n} = \frac{\rho_0(x_{m,s})^2}{2\rho_1} \left[\frac{n j_n(x_{m,c}) - x_{m,c} j_{n+1}(x_{m,c})}{(n-1)j_n(x_{m,c}) - x_{m,c} j_{n+1}(x_{m,c})} - \frac{2n(n+1)j_n(x_{m,s})}{(2n^2 - x_{m,s}^2 - 2)j_n(x_{m,s}) + 2x_{m,s} j_{n+1}(x_{m,s})} \right] \\ \times \left[\frac{(x_{m,s}^2/2 - n^2 + n)j_n(x_{m,c}) - 2x_{m,c} j_{n+1}(x_{m,c})}{(n-1)j_n(x_{m,c}) - x_{m,c} j_{n+1}(x_{m,c})} - \frac{2n(n+1)[(1-n)j_n(x_{m,s}) + x_{m,s} j_{n+1}(x_{m,s})]}{(2n^2 - x_{m,s}^2 - 2)j_n(x_{m,s}) + 2x_{m,s} j_{n+1}(x_{m,s})} \right]^{-1}, \quad (26)$$

where $x_{m,c} = (c_0/c_c)x_m$ and $x_{m,s} = (c_0/c_s)x_m$.

The solution for the rigid and movable sphere can be obtained by setting $c_c, c_s \rightarrow \infty$ in the previous discussion. The solution for liquid spheres is achieved by letting $c_s \rightarrow 0$.

B. Second-order ultrasound scattering

Before calculating the dynamic radiation force, we need to analyze the contribution of the second-order velocity potential in Eq. (22). The amplitude function $\hat{\phi}_{\Delta\omega}^{(2)}$ for an incident wave is calculated in the Appendix. In the pre-shock wave range, it is given by

$$\hat{\phi}_{\Delta\omega}^{(2)} = -\frac{\varepsilon v_0^2}{2\Delta\omega} j e^{-j\Delta k z}. \quad (27)$$

where $\varepsilon = 1 + B/(2A)$, v_0 is the peak amplitude of the velocity potential at the ultrasound source, and $\Delta k = \Delta\omega/c_0$. To simplify our analysis it was assumed that $\Delta k z \ll 1$. If the difference frequency is about 10 kHz, then the target should be around 1 cm of the ultrasound source.

Now, we need to solve the scattering problem for the second-order velocity potential. This problem is similar to the linear scattering presented in Sec. III A. Hence, the total second-order velocity potential amplitude can be written in spherical polar coordinates as

$$\hat{\phi}_{\Delta\omega}^{(2)} = -j \frac{\varepsilon v_0^2}{2\Delta\omega} \sum_{n=0}^{\infty} (2n+1)(-j)^n [j_n(\Delta k r) + S_n h_n^{(2)}(\Delta k r)] P_n(\cos \theta), \quad (28)$$

where the scattering function S_n is given through Eqs. (25) and (26) by setting $x_m = \Delta k r_0$.

According to Eq. (22) the contribution of the second-order velocity potential is given by integrating Eq. (28) over the sphere surface. This contribution to the dynamic radiation force has only one component in the z -direction given by

$$F_1 = -j 2\pi r_0^2 \rho_0 \Delta\omega \int_0^\pi \hat{\phi}_{\Delta\omega}^{(2)}(r_0) \sin \theta \cos \theta d\theta = -\pi r_0^2 E_0 \frac{4\varepsilon}{3} [j_1(\Delta k r_0) + S_1 h_1^{(2)}(\Delta k r_0)], \quad (29)$$

where $E_0 = (\rho_0 v_0^2)/2$ is ultrasound energy at the wave source.

C. Dynamic radiation force function

To calculate the dynamic radiation force we introduce the following variables $u_m = k_m r$ ($m = a, b$) and $v = \cos \theta$. By symmetry considerations the dynamic radiation force on the sphere is only in the z -direction. By substituting Eq. (24) into Eq. (22) leads to the amplitude of the dynamic radiation force as

$$\hat{f}_{\Delta\omega} = F_0 + F_1 + F_2 + F_3 + F_4 + F_5, \quad (30)$$

where the amplitude functions are

$$F_2 = -\pi r_0^2 \rho_0 k_a k_b \int_{-1}^1 \hat{\phi}_a(x_a, \nu) \hat{\phi}_b^*(x_b, \nu) \nu d\nu, \quad (31)$$

$$F_3 = -\pi r_0^2 \rho_0 k_a k_b \int_{-1}^1 \frac{\partial \hat{\phi}_a}{\partial u_a} \Big|_{u_a=x_a} \frac{\partial \hat{\phi}_b^*}{\partial u_b} \Big|_{u_b=x_b} \nu d\nu, \quad (32)$$

$$F_4 = \pi \rho_0 \int_{-1}^1 \frac{\partial \hat{\phi}_a}{\partial v} \Big|_{u_a=x_a} \frac{\partial \hat{\phi}_b^*}{\partial v} \Big|_{u_b=x_b} \nu (1 - \nu^2) d\nu, \quad (33)$$

$$F_5 = -\pi r_0 \rho_0 \int_{-1}^1 \left(k_a \frac{\partial \hat{\phi}_b^*}{\partial v} \Big|_{u_b=x_b} \frac{\partial \hat{\phi}_a}{\partial u_a} \Big|_{u_a=x_a} + k_b \frac{\partial \hat{\phi}_a}{\partial v} \Big|_{u_a=x_a} \frac{\partial \hat{\phi}_b^*}{\partial u_b} \Big|_{u_b=x_b} \right) (1 - \nu^2) d\nu, \quad (34)$$

and F_0 and F_1 are given by Eqs. (21) and (29), respectively.

To obtain the amplitude functions of the dynamic radiation force in Eq. (30), we substitute Eq. (24) into Eqs. (31)-(34), which leads to

$$F_2 = -\frac{2\pi r_0^2 E_{\Delta\omega}}{x_a x_b} \sum_{n=0}^{\infty} (n+1) x_a x_b (R_{a,n} R_{b,n+1}^* + R_{a,n+1} R_{b,n}^*), \quad (35)$$

$$F_3 = -\frac{2\pi r_0^2 E_{\Delta\omega}}{x_a x_b} \sum_{n=0}^{\infty} (n+1) x_a x_b (R'_{a,n} R_{b,n+1}^* + R'_{a,n+1} R_{b,n}^*), \quad (36)$$

$$F_4 = \frac{2\pi r_0^2 E_{\Delta\omega}}{x_a x_b} \sum_{n=0}^{\infty} n(n+1)(n+2) (R_{a,n} R_{b,n+1}^* + R_{a,n+1} R_{b,n}^*), \quad (37)$$

$$F_5 = \frac{2\pi r_0^2 E_{\Delta\omega}}{x_a x_b} \sum_{n=0}^{\infty} [n(n+1) (x_b R_{a,n} R_{b,n+1}^* + x_a R'_{a,n+1} R_{b,n}^*) - (n+1)(n+2) (x_a R'_{a,n} R_{b,n+1}^* + x_b R_{a,n+1} R_{b,n}^*)], \quad (38)$$

where $R_{m,n} = (-j)^n [j_n(x_m) + S_{m,n} h_n^{(2)}(x_m)]$ and $E_{\Delta\omega} = \rho_0 k_a k_b A_0^2$ is the difference frequency component of the ultrasound energy density.

Let us focus on the contribution of F_0 to the dynamic radiation force on the sphere. The magnitude of the velocity particle of the incident plane wave is $p_0/(\rho_0 c_0)$, where p_0 is the magnitude of the incident pressure. The magnitude of the velocity particle inside the object volume variation δV is smaller than its counter-part in the fluid. Hence, from Eq. (21) we have $|F_0| < \Delta\omega \delta M_{\max} p_0/(\rho_0 c_0)$, where δM_{\max} is the maximum amount of fluid mass dislocated by the sphere vibration. Measurements of the amplitude dislocation induced by the dynamic radiation force ($\Delta f < 1$ kHz, f_0 around 1 MHz, and $p_0 < 60$ kPa) on a stainless steel sphere of 1 mm diameter in water, yielded results less than $1 \mu\text{m}$ [36]. Now, we compare the magnitude of F_0 and F_2 . From Eq. (35) we have

$$\frac{|F_0|}{|F_2|} < \frac{\rho_0 f_0^2 \Delta f r_0^2 \delta r}{c_0 p_0},$$

where δr is the sphere radius variation. For the given condition of the experiment on measuring the dislocation amplitude of the sphere caused by the dynamic radiation force, the ratio $|F_0|/|F_1| \sim 10^{-2}$. In this case or whenever δr is negligible, only the components F_1 to F_5 are relevant to the radiation force formula (30).

One can show from Eq. (23) that the dynamic radiation force on the sphere in time-domain is

$$\mathbf{f}_{\Delta\omega}(t) = \pi r_0^2 E_{\Delta\omega} \Re \left\{ \hat{Y}_{\Delta\omega} e^{j\Delta\omega t} \right\} \mathbf{e}_z, \quad (39)$$

TABLE I: Physical constants used in the calculation of the radiation force functions.

Material	Density Kg/m ³	Speed of sound	
		Compressional m/s	Shear m/s
Brass	8100	3830	2050
Stainless steel	7670	5240	2978

where $\hat{Y}_{\Delta\omega}$ is the dynamic radiation force function given by

$$\begin{aligned} \hat{Y}_{\Delta\omega} = & -\frac{2}{x_a x_b} \sum_{n=0}^{\infty} (n+1) [(x_a x_b - n(n+2))(R_{a,n} R_{b,n+1}^* + R_{a,n+1} R_{b,n}^*) \\ & + n(x_b R_{a,n} R_{b,n+1}^* + x_a R_{a,n+1} R_{b,n}^*) - (n+2)(x_a R_{a,n} R_{b,n+1}^* + x_b R_{a,n+1} R_{b,n}^*) \\ & + x_a x_b (R_{a,n} R_{b,n+1}^* + R_{a,n+1} R_{b,n}^*)] - R_0, \end{aligned} \quad (40)$$

where $R_0 = \frac{4\epsilon E_0}{3E_{\Delta\omega}} [j_1(\Delta k r_0) + S_1 h_1^{(2)}(\Delta k r_0)]$.

The sphere is also subjected to a static radiation force, which is the sum of the force due to each ultrasound wave in the incident beam. The static radiation force on a spherical target has been calculated by Hasegawa [27]. The result reads

$$\mathbf{f}_s = \pi r_0^2 (E_a Y_a + E_b Y_b) \mathbf{e}_z,$$

where $E_m = \rho_0 (k_m A_0)^2 / 2$ ($m = a, b$). The quantity Y_m is the radiation pressure function given by

$$Y_m = -\frac{4}{x_m^2} \sum_{n=0}^{\infty} (n+1) (\alpha_{m,n} + \alpha_{m,n+1} + 2\alpha_{m,n} \alpha_{m,n+1} + 2\beta_{m,n} \beta_{m,n+1}), \quad m = a, b, \quad (41)$$

where $\alpha_{m,n}$ and $\beta_{m,n}$ are the real and the imaginary parts of $S_{m,n}$, respectively. Moreover, when $\Delta\omega = 0$ then $\hat{Y}_{\Delta\omega} = Y_m$.

Finally, the total radiation force exerted on the sphere by the dual-frequency plane wave is given by

$$\mathbf{f}_{\text{rad}}(t) = \pi r_0^2 \left(E_a Y_a + E_b Y_b + E_{\Delta\omega} \Re \left\{ \hat{Y}_{\Delta\omega} e^{j\Delta\omega t} \right\} \right) \mathbf{e}_z. \quad (42)$$

D. Numerical evaluation of the dynamic radiation force

The dynamic radiation force function $\hat{Y}_{\Delta\omega}$ was evaluated numerically in MATLAB 6.5 (MathWorks, Inc.). Two different materials were chosen in this evaluation: brass and stainless steel. The physical constants of the analyzed spheres are given in Table I. The surrounding fluid of the sphere was assumed to be water with density $\rho_0 = 1000 \text{ Kg/m}^3$, compressional velocity $c_0 = 1500 \text{ m/s}$. The radius of the sphere is $r_0 = 0.5 \text{ mm}$.

We are interested here in analyzing how the dynamic radiation force changes with the center frequency f_0 . We evaluate the function $\hat{Y}_{\Delta\omega}$ as a function of $k_0 r_0$ varying from 0.1 to 10. The difference frequency Δf was fixed to 0, 50, 100 kHz. To assure that the center frequency f_0 is always positive, we assume that f_0 varies from 50 kHz to 4.77 MHz.

Before presenting the numerical evaluation results, let us take a closer look to the contribution of the second-order velocity potential to the dynamic radiation force given in Eq. (29). For the frequency-range considered here, the energies E_0 and $E_{\Delta\omega}$ are about the same order of magnitude. In this case, the numerical evaluation of R_0 , see Eq. (40), for the chosen frequency-range has shown that the dimensionless amplitude of this quantity (10^{-3}) is much smaller than the unit. In fact, for the frequency range used in the simulations we have $\Delta k r_0 \ll 1$. Therefore, we may neglect the contribution of R_0 to the dynamic radiation force function given by Eq. (40) hereafter.

In Figs. 3 and 4, we see the magnitude of the dynamic radiation force function $|\hat{Y}_{\Delta\omega}|$. The inset of the figures shows the phase of $\hat{Y}_{\Delta\omega}$. We can see that when $\Delta f = 0$ the function $|\hat{Y}_{\Delta\omega}|$ of both materials is equal to the radiation

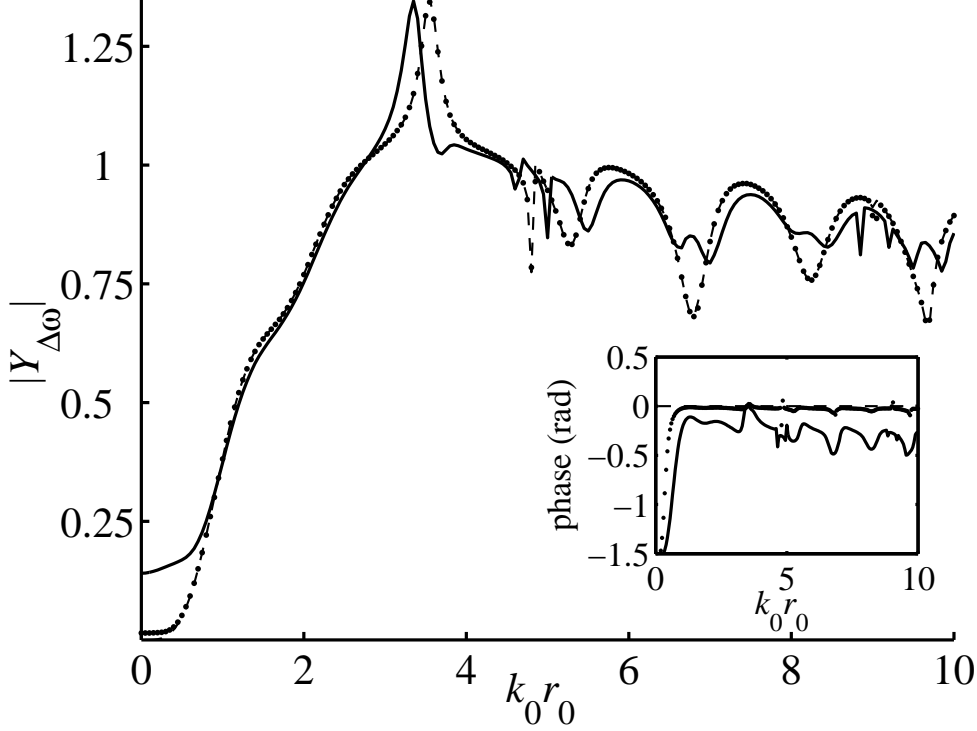


FIG. 3: Dynamic radiation force function of the brass sphere. The inset plot the phase of $\hat{Y}_{\Delta\omega}$. Legend: dashed line (0 kHz), dotted line (50 kHz), and solid line (100 kHz).

pressure function Y_m , as expected. The dynamic radiation force function of both material exhibits a fluctuation pattern (dips and peaks) due to resonances of the ultrasound wave inside the sphere. The fluctuations depend on resonances of the scattering function $S_{m,n}$, which is related to the material parameters (density, compressional and shear speed of the wave). No significant changes in $\hat{Y}_{\Delta\omega}$ (magnitude and phase) is observed as the difference frequency varies from 0 to 50 kHz. Further, the phase remains practically constant with zero value. This occurs because at 50 kHz we have $\Delta k r_0 = 0.02$, which implies $k_a r_0 \simeq k_b r_0$. Thus $\hat{Y}_{\Delta\omega}$ approaches to Y_m .

For the brass sphere, a prominent peak occurs in $|\hat{Y}_{\Delta\omega}|$ with $\Delta f = 0$ at $k_0 r_0 = 3.55$, as seen in Fig. 3. When the difference frequency is 100 kHz, the peak change its position to 3.27 and the whole fluctuation pattern changes. However, the fluctuation form follows that one of $\Delta f = 0$ with smaller amplitudes. The phase also presents fluctuation whose amplitude is approximately $\pi/6$ rad.

The function $|\hat{Y}_{\Delta\omega}|$ for the stainless steel sphere with $\Delta f = 0$ presents dips, as shown in Fig. 4. The first dips occurs at $k_0 r_0 = 5.17$. At $\Delta f = 100$ kHz, the fluctuations in $\hat{Y}_{\Delta\omega}$ have a different pattern with smaller amplitude compared to the case of $\Delta f = 0$. The phase of $\hat{Y}_{\Delta\omega}$ is practically constant when $\Delta f = 50$ kHz, except when $k_0 r_0 < 1$. For $\Delta f = 100$ kHz, the phase exhibits fluctuations with amplitude of about $\pi/6$ rad. The phase fluctuations follows the pattern exhibited in the magnitude of $\hat{Y}_{\Delta\omega}$.

Now we analyze how the dynamic radiation force changes as Δf varies. This is particularly useful to show possible resonances on the dynamic radiation force function of the spheres for a given center frequency f_0 . In Fig. 5, the function $|\hat{Y}_{\Delta\omega}|$ is plotted as Δf varies in from -100 kHz to 100 kHz. The phase of $\hat{Y}_{\Delta\omega}$ is shown in the inset of the figure. The frequency-range of Δf was chosen to reveal symmetry properties of $\hat{Y}_{\Delta\omega}$. We fixed $k_0 r_0$ to 3.55 and 4.82 for the dashed and solid lines, respectively. These values correspond to the first peak and dip, respectively, in Fig. 3. In both cases the $|\hat{Y}_{\Delta\omega}|$ is symmetric. The phase of $\hat{Y}_{\Delta\omega}$ is antisymmetric. Both magnitude and phase of $\hat{Y}_{\Delta\omega}$ change shape considerably as $k_0 r_0$ changes. The concavities of $|\hat{Y}_{\Delta\omega}|$ in Fig. 5 follow those shown in Fig. 3 for the resonance points 3.55 (peak) and 4.82 (dip).

The plot of the function $\hat{Y}_{\Delta\omega}$ of the stainless steel sphere as Δf varies from -100 kHz to 100 kHz is shown in Fig. 6. The inset of the figure plots the phase of $|\hat{Y}_{\Delta\omega}|$. The quantity $k_0 r_0$ was fixed at the first and second dips,

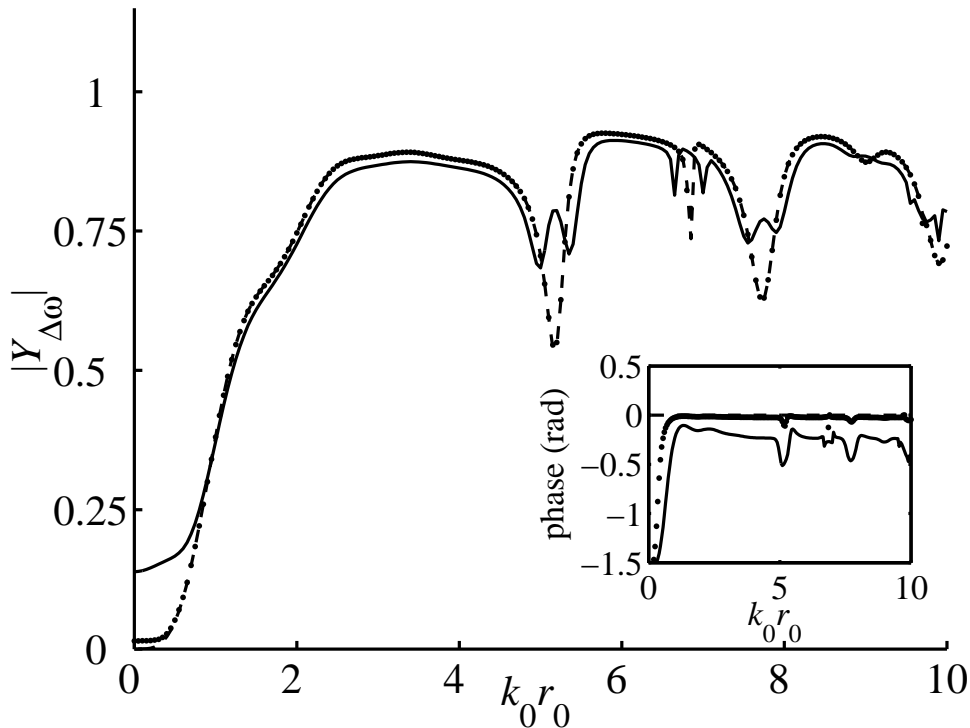


FIG. 4: Dynamic radiation force function of the stainless steel sphere. The inset plot the phase of $\hat{Y}_{\Delta\omega}$. Legend: dashed line (0 kHz), dotted line (50 kHz), and solid line (100 kHz).

which corresponds to 5.17 and 6.85 for the dashed and solid lines, respectively. The function $|\hat{Y}_{\Delta\omega}|$ for both values of $k_0 r_0$ exhibited a symmetric concave pattern. The phase showed an antisymmetric pattern in both cases. The concavities of $|\hat{Y}_{\Delta\omega}|$ seen in Fig. 6 follow those presented in Fig. 4 for points 5.17 and 6.85.

The comparison of the normalized amplitude of the static and the dynamic radiation forces on the stainless sphere as the center frequency varies can be seen in Fig. 7. The radiation force functions Y_a and Y_b are given by Eq. (41). The difference frequency was fixed to 10 kHz. The amplitudes are normalized by the highest ultrasound energy density E_a times the cross-section area of the sphere. In this figure, the solid line stands for the amplitude of the static radiation force, $Y_a + (k_b/k_a)^2 Y_b$. The dotted line corresponds to $(k_b/k_a)|\hat{Y}_{\Delta\omega}|$. The magnitude of the both radiation forces are about the same. Though we changed the difference frequency in a range up to 100 kHz, the magnitude of the static and the dynamic radiation force remained approximately the same.

IV. CONCLUSIONS

We have presented a theory to calculate the dynamic ultrasound radiation force exerted on an object by a dual-frequency CW ultrasound beam in lossless fluids. The theory is valid for beams with any spatial distribution. The amplitude of the induced vibration by the dynamic radiation force on the object was assumed to be much smaller than its characteristic dimensions. No assumptions have been made on geometric shape of the object. A formula for the dynamic radiation force was obtained – see Eq. (22) – in terms of the first- and second-order velocity potentials. The dependence of the dynamic radiation force with the nonlinear parameter B/A of the medium was analyzed.

We have calculated the dynamic radiation force exerted on a solid sphere by a dual-frequency CW plane wave in water. The dynamic radiation force is proportional to the cross-section area of the sphere, the dynamic ultrasound energy, and the dynamic radiation force function. The contribution of the first-order velocity potential to the radiation force, accounted by Eq. (30), was neglected because we considered that the dislocation of the sphere is very small. The contribution of the medium nonlinearity to the dynamic radiation force is negligible if $\Delta k r_0 \ll 1$

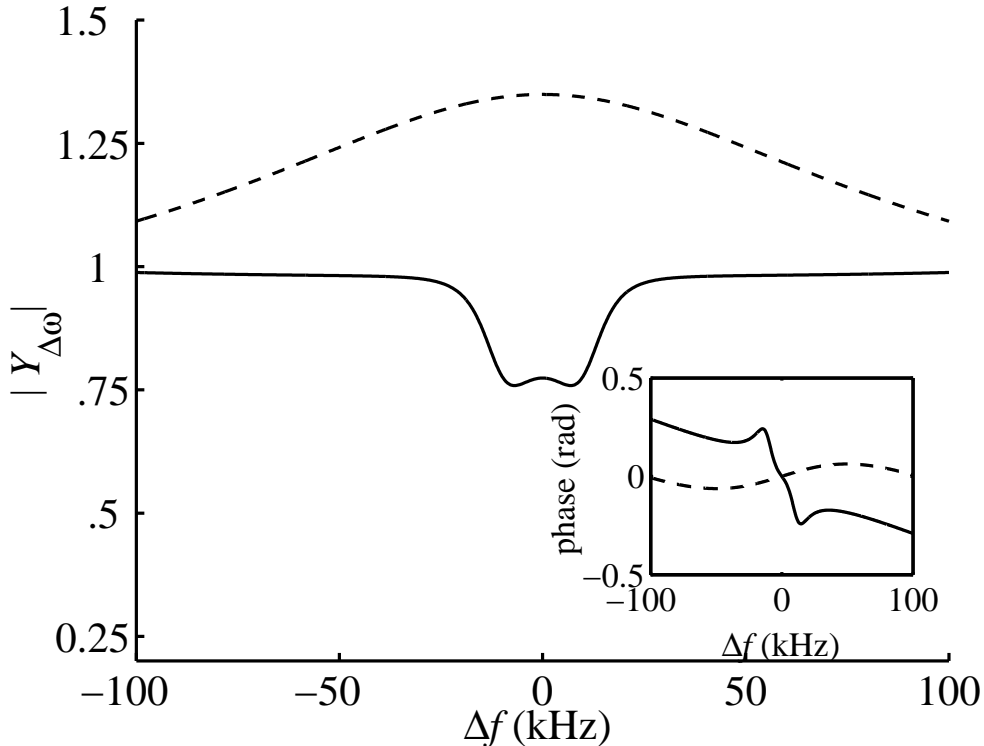


FIG. 5: Dynamic radiation force function as Δf varies for the brass sphere. Legend: dashed line ($k_0 r_0 = 3.55$) and solid line ($k_0 r_0 = 4.82$).

in a weak nonlinear medium. However, it may become more significant in strongly nonlinear mediums or when $\Delta k r_0 \sim 1$. Numerical evaluation of the dynamic radiation force function revealed a fluctuation pattern as the center frequency varies. The fluctuations are similar to those present in the static radiation force function. Analysis of the static and the dynamic radiation force on the sphere has shown that they have approximately the same magnitude. Experimental measurements of the magnitude of the static and the dynamic radiation force on a stainless steel sphere have confirmed this prediction [36].

In conclusion, the presented dynamic radiation force formula (22) generalizes Yosioka's formula [23], which stands only for the static radiation force. The dynamic radiation force formula can be extended for a multi-frequency CW ultrasound beam. This is particularly useful to study pulsed radiation force in which the incident ultrasound beam can be expanded in time as a Fourier series.

Acknowledgments

This work was partially supported by grant DCR013.2003-FAPEAL/CNPq (Brazil).

APPENDIX A: SECOND-ORDER VELOCITY POTENTIAL

To calculate the contribution of the second-order velocity potential to the dynamic radiation force on the sphere, we consider the lossless Burger's equation

$$\frac{\partial v}{\partial z} - \frac{\varepsilon}{c_0^2} v \frac{\partial v}{\partial \tau} = 0,$$

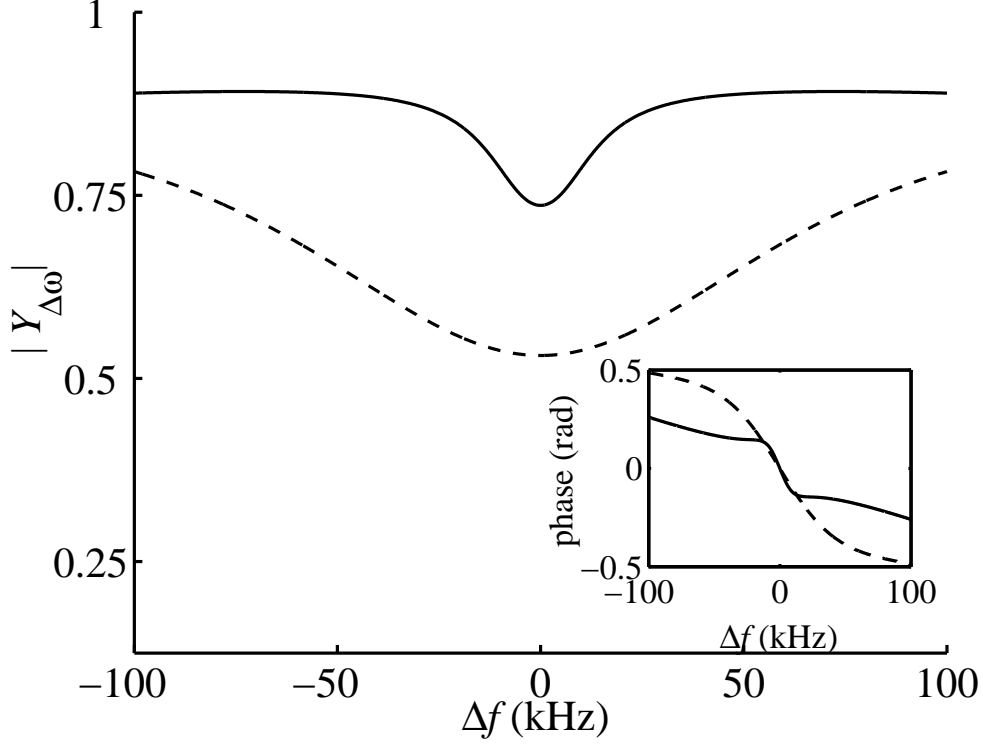


FIG. 6: Dynamic radiation force function as Δf varies for the stainless steel sphere. Legend: dashed line ($k_0 r_0 = 5.17$) and solid line ($k_0 r_0 = 6.85$).

where v is the velocity particle in the z -direction, $\varepsilon = 1 + B/(2A)$, and $\tau = t - z/c_0$ is the retarded time. The source wave form is given by

$$v(0, \tau) = v_0[\sin(\omega_a \tau) + \sin(\omega_b \tau)],$$

where v_0 is the peak amplitude of the velocity particle at the wave source ($z = 0$). Hence, the second-order velocity particle at the difference frequency in the pre-shock wave range is given by [37]

$$v_{\Delta\omega}^{(2)} \simeq -\frac{\varepsilon v_0^2}{2c_0} \Delta k z \sin(\Delta\omega t - \Delta k z),$$

This approximated solution is valid for $\varepsilon v_0 \Delta k z / c_0 \ll 1$. We obtain the second-order velocity potential at the difference frequency by integrating this equation over z . Thus, in complex notation, the amplitude of the velocity potential at $\Delta\omega$ is

$$\hat{\phi}_{\Delta\omega}^{(2)} = \frac{\varepsilon v_0^2}{2\Delta\omega} (\Delta k z - j) e^{-j\Delta k z}.$$

Notice that the time-dependent integration constant was dropped because it evaluates zero in the closed surface integral of Eq. (22).

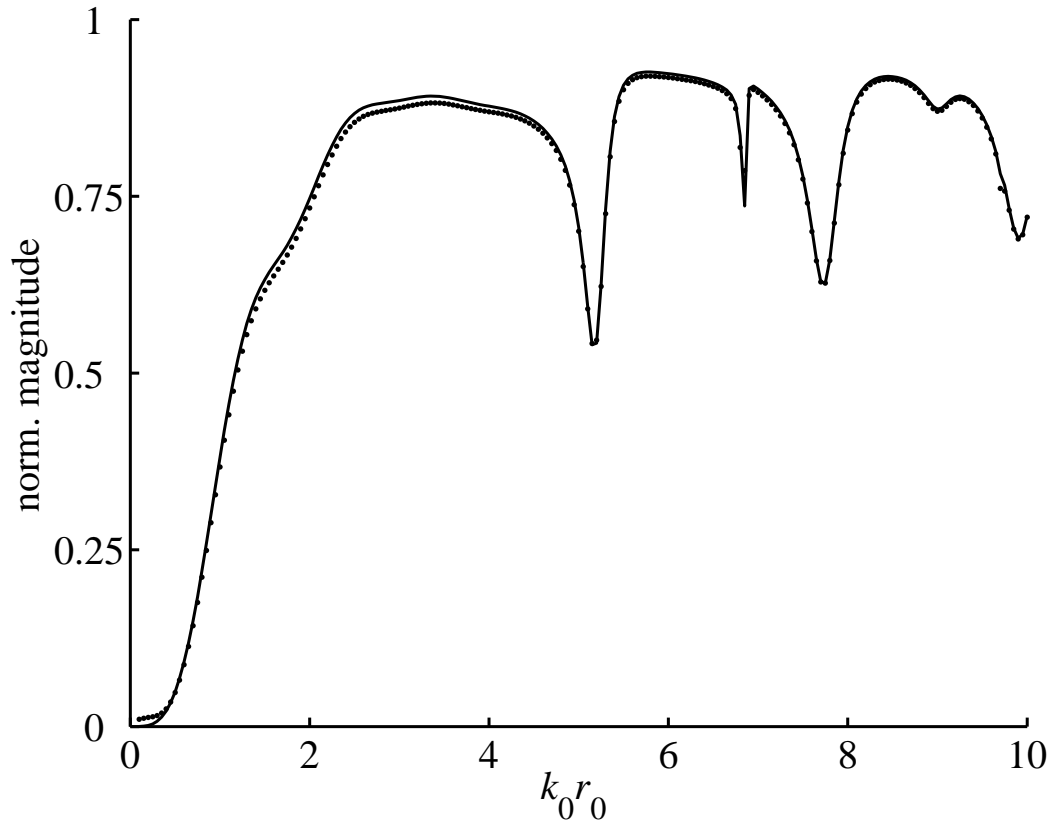


FIG. 7: Comparison on the magnitude of the static and the dynamic ultrasound radiation force on the stainless steel sphere with $\Delta f = 10$ kHz. Legend: dotted line represents $(k_b/k_a)|\hat{Y}_{\Delta\omega}|$ and solid line stands for $Y_a + (k_b/k_a)^2 Y_b$.

-
- [1] F. E. Borgnis, Rev. Mod. Phys. **25**(3), 653 (1953).
 - [2] R. T. Beyer, J. Acoust. Soc. Am. **63**(4), 1025 (1978).
 - [3] G. R. Torr, Am. J. Phys. **52**(5), 402 (1984).
 - [4] C. P. Lee and T. G. Wang, J. Acoust. Soc. Am. **94**(2), 1099 (1993).
 - [5] P. L. Carson, P. R. Fischella, and T. V. Oughton, Ultrasound Med. Biol. **3**, 341 (1978).
 - [6] R. C. Chivers and L. W. Anson, J. Acoust. Soc. Am. **72**(6), 1695 (1982).
 - [7] C. P. Lee, A. Anilkumar, and T. G. Wang, Phys. Fluids A **3**(11), 2497 (1991).
 - [8] L. A. Crum and A. Prosperetti, J. Acoust. Soc. Am. **73**(1), 121 (1983).
 - [9] L. J. Sivian, Philos. Mag. J. Sci. **5**(7), 615 (1928).
 - [10] M. Greenspan, F. R. Breckenridge, and C. E. Tschiegg, J. Acoust. Soc. Am. **63**(4), 1031 (1978).
 - [11] F. L. McNamara and R. T. Beyer, J. Acoust. Soc. Am. **25**(2), 259 (1952).
 - [12] K. Nightingale, M. S. Soo, R. Nightingale, and G. Trahey, Ultrasound Med. Biol. **28**(2), 227 (2002).
 - [13] A. P. Sarvazyan, O. V. Rudenko, S. D. Swanson, J. B. Fowlkes, and S. Y. Emelianov, Ultrasound Med. Biol. **24**(9), 1419

(1998).

- [14] M. Fatemi and J. F. Greenleaf, *Sci.* **280**, 82 (1998).
- [15] M. Fatemi and J. F. Greenleaf, *Proc. Nat. Acad. Sci. USA* **96**, 6603 (1999).
- [16] S. Chen, M. Fatemi, and J. F. Greenleaf, *J. of the Acoust. Soc. Am.* **112**(3), 884 (2002).
- [17] L. Rayleigh, *Philos. Mag.* **3**, 338 (1902).
- [18] Z.-Y. Jiang and J. F. Greenleaf, *J. Acoust. Soc. Am.* **100**(2), 741 (1996).
- [19] A. A. Doinikov, *Phys. Rev. E* **54**(6), 6297 (1996).
- [20] S. D. Danilov and M. A. Mironov, *J. Acoust. Soc. Am.* **107**(1), 143 (2000).
- [21] J. H. Cantrell, *Phys. Rev. B* **30**, 3214 (1984).
- [22] L. V. King, *Proc. R. Soc. London* **147**(861), 212 (1934).
- [23] K. Yosioka and Y. Kawasima, *Acustica* **5**, 167 (1955).
- [24] P. J. Westervelt, *J. Acoust. Soc. Am.* **29**(1), 26 (1957).
- [25] G. Maidanik and P. J. Westervelt, *J. Acoust. Soc. Am.* **29**, 936 (1957).
- [26] L. P. Gor'kov, *Sov. Phys – Dokl.* **6**(9), 773 (1962).
- [27] T. Hasegawa and K. Yosioka, *J. Acoust. Soc. Am.* **46**, 1139 (1969).
- [28] T. Hasegawa, K. Saka, N. Inoue, and K. Matsuzawa, *J. Acoust. Soc. Am.* **83**(5), 1770 (1988).
- [29] L. Landau and E. Lifshitz, *Fluid Mechanics*, (Butterworth-Heinemann, Oxford, 1987), Ch. 1.
- [30] F. E. Fox and W. A. Wallace, *J. Acoust. Soc. Am.* **26**(6), 994 (1954).
- [31] H. Olsen, W. Roberg, and H. Wegerland, *J. Acoust. Soc. Am.* **30**(1), 69 (1958).
- [32] G. E. Mase, *Theory and Problems of Continuum Mechanics* (McGraw-Hill, New York, 1970), p.4.
- [33] J. Lighthill, *Waves in Fluids* (Cambridge University Press, Cambridge, 1978), p.337.
- [34] E. L. Lima, *Course of Analysis*, (Instituto de Matemática Pura e Aplicada, Rio de Janeiro, 1981), p.370 [in Portuguese].
- [35] J. J. Faran, *J. Acoust. Soc. Am.* **23**, 405 (1951).
- [36] S. Chen, G. T. Silva, M. Fatemi, and J. F. Greenleaf (to be published).
- [37] F. H. Fenlon, *J. Acoust. Soc. Am.* **51**(1), 284 (1972).